YjeQ, an Essential, Conserved, Uncharacterized Protein from *Escherichia coli*, Is an Unusual GTPase with Circularly Permuted G-Motifs and Marked Burst Kinetics†

Denis M. Daigle,‡ Laura Rossi,‡ Albert M. Berghuis,‡ L. Aravind,§ Eugene V. Koonin,§ and Eric D. Brown*,‡

Antimicrobial Research Centre, Department of Biochemistry, McMaster University, Hamilton, Ontario, Canada L8N 3Z5, and National Center for Biotechnology Information, National Institutes of Health, Room 8N805, Building 38A, 8600 Rockville Pike, Bethesda, Maryland 20894

Received May 15, 2002; Revised Manuscript Received July 14, 2002

ABSTRACT: The *Escherichia coli* protein YjeQ represents a protein family whose members are broadly conserved in bacteria and have been shown to be indispensable to the growth of *E. coli* and *Bacillus subtilis* [Arigoni, F., et al. (1998) *Nat. Biotechnol. 16*, 851]. Proteins of the YjeQ family contain all sequence motifs typical of the vast class of P-loop-containing GTPases, but show a circular permutation, with a G4−G1−G3 pattern of motifs as opposed to the regular G1−G3−G4 pattern seen in most GTPases. All YjeQ family proteins display a unique domain architecture, which includes a predicted N-terminal OB-fold RNA-binding domain, the central permuted GTPase module, and a zinc knuckle-like C-terminal cysteine cluster. This domain architecture suggests a possible role for YjeQ as a regulator of translation. YjeQ was overexpressed, purified to homogeneity, and shown to contain 0.6 equiv of GDP. Steady state kinetic analyses indicated slow GTP hydrolysis, with a k_{cat} of 9.4 h^{-1} and a K_m for GTP of 120 μM (k_{cat}/K_m = 21.7 M^{-1} s^{-1}). YjeQ also hydrolyzed other nucleoside triphosphates and deoxynucleotide triphosphates such as ATP, ITP, and CTP with specificity constants (k_{cat}/K_m) ranging from 0.2 to 1.0 M^{-1} s^{-1}. Pre-steady state kinetic analysis of YjeQ revealed a burst of nucleotide hydrolysis for GTP described by a first-order rate constant of 100 s^{-1} as compared to a burst rate of 0.2 s^{-1} for ATP. In addition, a variant in the G1 motif of YjeQ (S221A) was substantially impaired for GTP hydrolysis (0.3 s^{-1}) with a less significant impact on the steady state rate (1.8 h^{-1}). In summary, *E. coli* YjeQ is an unusual, circularly permuted P-loop-containing GTPase, which catalyzes GTP hydrolysis at a rate 45 000 times greater than that of turnover.

GTPases function as crucial molecular switches in a broad variety of biochemical processes. The majority of GTPases form a vast class of evolutionarily related proteins within the superclass of P-loop-containing ATPases (*1*, *2*). The P-loop GTPases share a common structural core exemplified by the structurally characterized GTPase domains of the Ras protein (*3*−*5*). A considerable depth of biochemical investigation of GTPases, particularly the Ras family, the α-subunits of heterotrimeric G-proteins, and the translation elongation factors EF-Tu and EF-G, has revealed a number of structural and functional generalizations. Principal among those are a conserved amino acid sequence G1−G3−G4 motif pattern (G2 is a less conserved motif found only in some GTPases) present in the GTPase domain (*3*) and a reputation for inefficient catalysis of GTP hydrolysis. The latter is rooted in a signaling paradigm where the rates of GTP hydrolysis and product release define the lifetime of GTP- and GDP-bound complexes, and consequently the regulatory states of G-proteins.

The *Escherichia coli* protein YjeQ represents a protein family whose members are broadly conserved in bacteria and have been shown to be indispensable to the growth of *E. coli* and *Bacillus subtilis* (*6*). In most public databases, such as GenBank and SWISS-PROT, YjeQ has been annotated as a potential ATP-binding protein. However, a more detailed examination of the sequence alignment of this family, which was performed during the construction of the Clusters of Orthologous Groups (COGs) protein database (*7*, *8*), revealed all diagnostic motifs of the P-loop GTPases, albeit in an unusual arrangement. Specifically, YjeQ and its orthologs exhibit an altered connectivity described by a G4−G1−G3 pattern, indicative of a circular permutation of the classic GTPase domain. Protein engineering experiments have frequently demonstrated that, provided protein termini are proximal in the native structure, circular permutation of enzymes can be accomplished without loss of function (*9*). In contrast, observations of circular permutation of proteins in the actual evolution of protein families have been relatively rare and only recently documented. Well-explored examples include swaposins (*10*) and certain families of DNA methylases (*11*, *12*). A plausible scenario for evolution of circular permutation in proteins has been proposed whereby the process starts with a duplication of the domain in question and proceeds by N- and C-terminal truncation, yielding a permutation (*10*). In the work described here, we report that YjeQ is an unusual, circularly permuted GTPase that

† This work was supported by a research grant from The Althexis Co. (Waltham, MA), the Ontario Innovation Trust, the Canadian Foundation for Innovation, and a Canada Research Chair to E.D.B.

* To whom correspondence should be addressed. Antimicrobial Research Center, Department of Biochemistry, McMaster University, 1200 Main Street West, Hamilton, Ontario, Canada, L8N 3Z5. Phone: (905) 525−9140 ext 22392 Fax: (905) 522−9033 Email: ebrown@mcmaster.ca.

‡ McMaster University.

§ National Institutes of Health.

10.1021/bi020355q CCC: $22.00
Published on Web 08/23/2002

catalyzes rapid hydrolysis of GTP with comparatively slow catalytic turnover.

MATERIALS AND METHODS

Sequence and Structure Analysis. The nonredundant protein sequence database (National Center for Biotechnology Information, National Institutes of Health) was searched using the gapped version of the BLASTP program (*13*). Iterative sequence profile searches were performed using the PSI-BLAST program (*13*). Multiple alignments of amino acid sequences were generated using a combination of the PSI-BLAST and T_Coffee (*14*) programs. The three-dimensional structure visualization and alignment were carried out using the SWISS-PDB-Viewer program, and modeling was accomplished by submitting the alignments of the template and the target to the SWISS-MODELLER server that utilizes the PROMODII program, via the SWISS-PDB-Viewer (*15*). Ribbon diagrams were generated using Molscript (*16*).

Construction of Overexpression Clones. The *yjeQ* gene was PCR amplified from *E. coli* MG1655 chromosomal DNA using the polymerase chain reaction. Amplification was performed using VENT DNA polymerase (New England Biolabs, Beverly, MA) and the following primers: 5′-GCG CGG GAA TTC CAT ATG AGT AAA AAT AAA CTC TCC AAA GG-3′and 5′-CGC GGA TCC TCA GTC ATC CGT ATC AGA AAA G-3′. The underlined sequences denote restriction sites for *Nde*I, incorporating the start codon, and *Bam*HI, flanking the stop codon. The resulting product was digested with *Nde*I and *Bam*HI and ligated to *Nde*I- and *Bam*HI-digested plasmid pBF-9, a derivative of pKK223-3 (Stratagene) that has been described previously (*17*). The resulting construct (pLR1) was sequenced to confirm the authenticity of the inserted gene by MOBIX (McMaster University). A His-tagged version of YjeQ was also made using the Gateway phage lambda site specific recombination system (Invitrogen Canada, Burlington, ON) according to the manufacturer's instructions. In short, the *yjeQ* gene was cloned by PCR (5′-G GGG ACA AGT TTG TAC AAA AAA GCA GGC TTA AGT AAA AAT AAA CTC TCC AAA GGC-3′ and 5′-G GGG ACC ACT TTG TAC AAG AAA GCT GGG TCT CAG TCA TCC GTA TCA GAA AAG TTT TTA CGC G-3′, recombination sequences underlined) into entry plasmid pENTR1A (Gateway cloning manual) and subsequently moved to pDEST17, a T7 expression vector that incorporated six histidines and a linker sequence at the N-terminus of YjeQ. The insert of the resulting overexpression construct (pDEST17-YjeQ) was confirmed by sequencing (MOBIX, McMaster University).

Variant Ser221Ala of YjeQ was constructed using QuickChange Site Directed Mutagenesis Kit (Stratagene, La Jolla, CA) and plasmid PLR-1 according to the manufacturer's instructions (primers 5′-TGG CGT CGG CAA AGC CAG CCT GCT GAA TGC-3′ and 5′-GCA TTC AGC CTG GCT TTG CCG ACG CCA-3′, sites of mutagenesis underlined). The insert of the resulting overexpression construct (pLR1-S221A) was confirmed by sequencing (MOBIX, McMaster University). This procedure was also employed to make histidine-tagged variants Lys220Ala (primers 5′-GTC TGG CGT CGG CGC TAG CAG CCT GCT GAA TGC G-3′ and 5′-CGC ATT CAG CAG GCT GCT AGC GCC GAC GCC AGA C-3′, sites of mutagenesis underlined), Ser221Ala (primers 5′-TGG CGT CGG CAA AGC CAG CCT GCT GAA TGC-3′ and 5′-GCA TTC AGC AGG CTG GCT TTG CCG ACG CCA-3′, sites of mutagenesis underlined), and Lys220Ala/Ser221Ala (primers 5′-GTC TGG CGT CGG CGC TGC TAG CCT GCT GAA TGC G-3′ and 5′-CGC ATT CAG CAG GCT AGC AGC GCC GAC GCC AGA C-3′, sites of mutagenesis underlined) using plasmid pDEST17-YjeQ. The inserts of the resulting overexpression constructs [pDEST17-YjeQ(K220A), pDEST17-YjeQ(S221A), and pDEST17-YjeQ(K220A/S221A] were confirmed by sequencing (MOBIX, McMaster University).

Protein Purification. Native untagged YjeQ was purified from *E. coli* W3110 cells, freshly transformed with pLR-1. Cells were grown (37 °C) in Luria-Bertani medium (6 × 1 L) supplemented with 50 μg/mL ampicillin to an optical density (595 nm) of 0.4. The culture was then induced with isopropyl β-thiogalactoside (1 mM), grown to an optical density of 1.1, harvested, and washed (0.85% NaCl) by centrifugation (8000*g* for 10 min). All subsequent purification steps were carried out at 4 °C. Cells were resuspended in 30 mL of lysis buffer [50 mM Hepes (pH 7.5) with 1 mM DTT, 1 mM phenylmethanesulfonyl fluoride, and 1 mM EDTA] and were disrupted with three consecutive passes through a French press at 20 000 psi. The lysate was clarified by centrifugation at 72000*g*, loaded onto a Q-Sepharose Fast Flow (Amersham-Pharmacia, Baie d'Urfé, PQ) anion exchange column (2.6 cm × 12 cm), and washed with 150 mL of 50 mM Hepes (pH 7.5) and 1 mM DTT. Proteins were eluted with a linear gradient from 0 to 1 M NaCl in 900 mL. SDS−polyacrylamide gel electrophoresis indicated that fractions containing YjeQ eluted with approximately 0.35−0.4 M NaCl. These fractions were pooled and concentrated to 20 mL, using an Amicon 8200 stirred cell concentrator and PM30 membranes (Fisher Scientific, Napean, ON) before concentration to 1 mL with Millipore Ultrafree-15 Centrifugal Filters (Fisher Scientific, Napean, ON). The concentrated sample (1 mL) was chromatographed on a Superdex S75 (Amersham-Pharmacia) gel filtration column (1.6 cm × 64 cm). Fractions judged to be greater than 98% pure by SDS−polyacrylamide gel electrophoresis were pooled (yield of typically 125 mg/L), concentrated to a final concentration of 60 mg/mL, and stored at −80 °C. Confirmation of the identity of the purified YjeQ was accomplished by N-terminal amino acid sequencing of the first 10 amino acids (Alberta Peptide Institute, Edmonton, AB). The Ser221Ala variant of YjeQ was similarly prepared from *E. coli* W3110 transformed with pLR1-S221A.

His-tagged YjeQ and His-tagged variants of YjeQ were purified from *E. coli* BL21(DE3) freshly transformed with pDest17-YjeQ, pDEST17-YjeQ(K220A), pDEST17-YjeQ-(S221A), or pDEST17-YjeQ(K220A/S221A). Cells (4 × 1 L) were grown (37 °C) in Luria-Bertani broth to an optical density of 0.25, induced with isopropyl β-thiogalactoside (1 mM), and grown for an additional 3 h. The cells were harvested by centrifugation, lysed, and clarified in 50 mM Hepes, 500 mM NaCl, and 15 mM imidazole (pH 7.5). The clarified lysate was loaded onto an Amersham-Pharmacia HiTrap chelating column (0.7 cm × 2.5 cm) preloaded with 0.5 mL of 100 mM $NiCl_2$. The column was developed with a linear gradient of 15 to 300 mM imidazole in 56 mL in the buffer described, and fractions containing His-tagged

YjeQ were pooled and concentrated using an Amicon 8200 stirred cell concentrator and PM30 membranes (Fisher Scientific) before concentration to 1 mL with Millipore Ultrafree-15 Centrifugal Filters (Fisher Scientific). The 1 mL sample was separated into four 250 μL injections onto a Pharmacia analytical Sephadex S200 gel filtration column equilibrated in running buffer [50 mM Hepes (pH 7.5), 1 mM DTT, and 150 mM NaCl]. Fractions from all four separate runs were pooled and chromatographed over a Pharmacia 1 mL Mono Q anion exchange column. Proteins were eluted with a linear gradient from 0 to 1 M NaCl in 65 mL. Pure His-tagged YjeQ eluted between 0.3 and 0.37 M was concentrated and buffer exchanged [the final buffer being 50 mM Hepes (pH 7.5), 50 mM NaCl, and 15% glycerol] to 10 mg/mL and stored at −80 °C. Protein concentrations of tagged and untagged purified YjeQ and variants were determined according to the method of Gill and von Hippel (*18*).

To test for copurification of contaminating nucleoside triphosphate hydrolases, we also carried out mock purifications of tagged and untagged YjeQ. The mock purifications were performed exactly as described above with the exception that *E. coli* W3110 and BL21(DE3) were transformed with plasmids lacking the gene *yjeQ*, namely, pKK233-3** (*17*) and pET22b, respectively. Great care was taken in these mock protocols to collect exactly the same fractions during chromatography steps and to concentrate all fractions to the same volumes used in the standard purification and assay protocols.

GTP Binding Assay. Binding of [^{35}S]GTPγS to purified YjeQ was assayed using a standard filter binding assay (*19*) followed by liquid scintillation counting of the washed filters. In a 500 μL volume, YjeQ (10.9 μM) and [^{35}S]GTPγS (500 μM, 36.4 Ci/mol) were incubated for 2 h at 30 °C in assay buffer [50 mM Hepes (pH 8), 10 mM $MgCl_2$, and 40 mM KCl]. Incubations were terminated with the addition of 2.5 mL of ice-cold assay buffer and filtered through Whatman GF/C Glass Microfiber Filters (VWR Canlab, Mississauga, ON) using a Millipore 1225 Filtration Sampling Manifold (VWR Canlab).

Steady State Assays of Nucleotide Hydrolysis. Catalysis of nucleotide hydrolysis by pure YjeQ was assessed through measurement of the amount of inorganic phosphate produced using a standard malachite green/ammonium molybdate colorimetric assay (*20*) and additionally by analysis of the product GDP by reverse phase HPLC. In all assays, YjeQ concentrations were less than one-tenth of that of the lowest concentration of nucleotide substrate [50 mM Hepes (pH 7.5) and 10 mM $MgCl_2$], where substrate concentrations ranged from 10 μM to 10 mM. Initial rates were measured from reactions (50 μL) that were allowed to proceed for up to 4 h at room temperature (23 °C) before being quenched with malachite green/ammonium molybdate reagent for phosphate analysis or by base (final concentration of 0.2 N NaOH) prior to analysis using HPLC on a Waters (Milford, MA) 600 chromatography system with Millenium analysis software. HPLC employed paired ion chromatography (*21*) using a C-18 reverse phase column (15 cm × 4.6 mm, Regis Reversible Spherisorb S50DS, Sigma, Mississauga, ON) and a gradient of the following buffers: (A) 100 mM sodium phosphate (pH 6) and 10 mM tetrabutylammonium hydrogen sulfate and (B) 7:3 mixture of buffer A and methanol (pH adjusted to 7.2 with NaOH). For separation, we used the following method parameters: 5 min in buffer A, a 1 min linear gradient to 100% B, and 100% B for 6 min (flow rate of 1 mL/min).

Rapid Quench Experiments. Rapid mixing of YjeQ and substrates employed a BioLogic Quenched Flow SFM-400 mixer and MPS-52 controller (Molecular Kinetics, Seattle, WA). Experiments were performed at room temperature (23 °C) in buffer containing 50 mM Hepes (pH 7.5) and 10 mM $MgCl_2$. For mixing experiments, a three-syringe method was used where 112 μL of substrate (e.g., 5 mM [α-^{32}P]GTP, 4 Ci/mol) was mixed with 112 μL of enzyme (800, 1200, 1600, or 2200 μM) and allowed to react for 2.3 ms to 120 s before the reaction was quenched with the addition of 112 μL of 0.6 N NaOH. Quenched samples were filtered prior to HPLC to remove denatured protein using Amicon Ultrafree-MC filters (Fisher Scientific) with a 5000 Da cutoff. Production of [α-^{32}P]GDP was monitored by paired ion chromatography (described above) with in-line radioactivity detection (Flow Scintillation Analyzer 150TR from Packard, Meriden, CT). The time course of GTP hydrolysis was fit to the biphasic burst equation:

$$Y = a[1 - \exp(-k_1 t)] + k_2 t \quad (1)$$

where a is the amplitude of the burst representing the formation of GDP·P_i at the active site, k_1 is the rate constant of the pre-steady state burst phase, k_2 is the steady state rate, and t is the time in seconds.

RESULTS

Analysis of the Sequence and Structure of YjeQ. Analysis of the protein sequences of YjeQ and its orthologs revealed three discrete regions that probably correspond to structural domains: an N-terminal (residues 10−117) S1-like OB-fold RNA-binding domain, a central GTPase domain (residues 121−271), and a *C*-terminal domain, which contains a cluster of conserved cysteines and a histidine, which is predicted to bind a divalent metal ion (possibly zinc) and was termed ZF (Zn finger) (Figure 1A).

The N-terminal portion of YjeQ showed a low but statistically significant level of sequence similarity with respect to a variety of protein domains of the S1-like family of OB-folds (*22*, *23*). For example, when an iterative database search was initiated with the sequence of the 125 N-terminal residues of YjeQ and the profile inclusion cutoff set at 0.02, the sequence of the translation initiation factor eIF1 from *Pyrococcus horikoshii*, a typical OB-fold protein, was detected in the third iteration with a random expectation value of ~0.01. Secondary structure prediction using a multiple alignment of the predicted S1-like OB fold revealed the presence of five conserved β-strands and conserved hydrophobic residues typical of the S1-like OB-fold (Figure 1B). This strongly suggested that the N-terminal parts of the YjeQ family proteins adopted this fold. S1-like OB folds are found in various RNA-binding proteins, such as translation factors, transcription factors, and regulators of mRNA metabolism. The structure of the OB-fold from ribosomal protein S1 shows a five-stranded β-barrel structure that interacts with single-stranded nucleic acids through a deep cleft (*23*). The presence of this predicted RNA-binding domain in YjeQ points to a potential role for this protein in RNA metabolism.

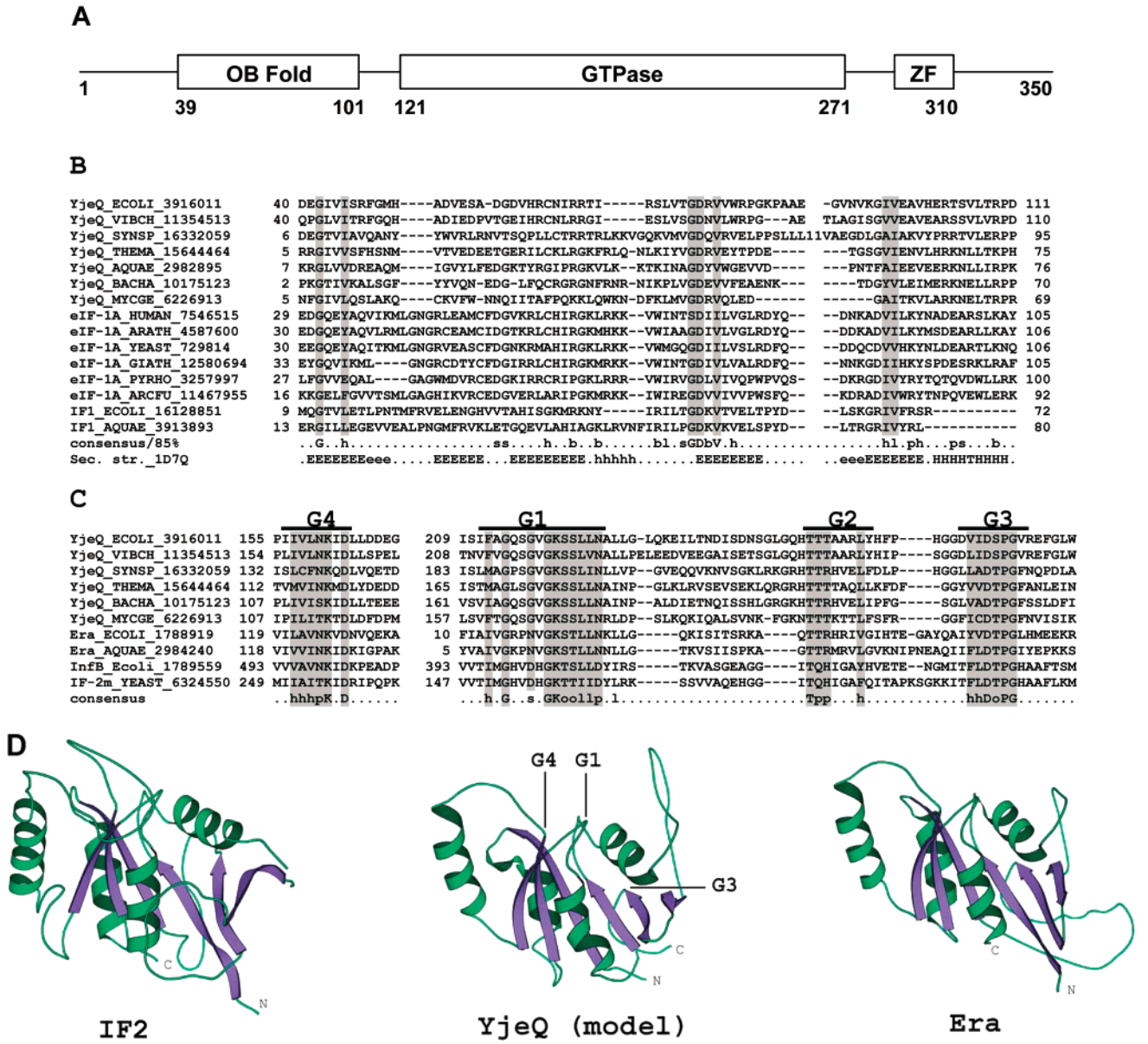

FIGURE 1: Sequence analysis and homology modeling of *E. coli* YjeQ. Panel A depicts a scaled diagram of the domain structure of YjeQ (SWISSPROT entry P39286) as revealed by sequence analysis. An N-terminal S1/PNP OB-fold (*22*), a central Ras-like GTPase domain (*1*−*3*), and a C-terminal Zn cluster with three conserved cysteines and a conserved histidine (CCHC) are shown. Panel B shows the alignment of the predicted N-terminal, S1-like OB-fold domain of YjeQ family proteins with a selection of functionally characterized OB-fold domains of this class from translation initiation factors. The secondary structure is from the NMR structure of the human translation initiation factor 1α (PDB entry 1D7Q). E indicates extended conformation (*β*-strand), and H indicates α-helix. Lowercase letters indicate poorly conserved structural elements. The consensus includes amino acid residues that are conserved in at least 85% of the aligned sequences; h stands for hydrophobic residues (ACVILMFYW), l for aliphatic residues (AVIL), s for small residues (GASTVDN), b for big residues (ILMFYWEQKR), and p for polar residues (STKRHEDNQ). The residues conserved in all aligned sequences are shaded. The numbers preceding and succeeding the aligned sequences indicate the positions of the first and last amino acid residues, respectively, in the corresponding protein. Each protein is denoted by its name, abbreviated species name, and the Gene Identifier (GI number) from the GenBank database. Species abbreviations: ECOLI, *E. coli*; VIBCH, *Vibrio cholerae*; SYNSP, *Synechocystis* sp.; THEMA, *Thermotoga maritima*; AQUAE, *Aquifex aeolicus*; BACHA, *Bacillus halodurans*; MYCGE, *Mycoplasma genitalium*; ARATH, *Arabidopsis thaliana*; YEAST, *Saccharomyces cerevisiae*; GIATH, *Guillardia theta*; PYRHO, *Pyrococcus horikoshii*; and ARCFU, *Archaeoglobus fulgidus*. Panel C shows the alignment of the conserved regions of the GTPase domain of YjeQ family proteins with the corresponding regions of two structurally and functionally characterized GTPases involved in translation, Era and initiation factor 2 (IF2). The four conserved motifs characteristic of GTPases are marked. The numbers indicate the positions of the first residue of each of the aligned blocks in the corresponding protein sequences. The order of the blocks is as in the YjeQ family proteins so that the blocks in Era and IF2 are permuted (see the text). The consensus shows residues that are conserved in all aligned sequences. The remaining designations are as described for panel A. Panel D displays ribbon diagrams (*16*, *24*, *35*) of the refined structures of translation factor IF2 (PDB entries 1G7S and 1G7T) and Era GTPase (PDB entry 1EGA) and a homology model of the core GTPase domain of YjeQ, which was generated using these two structures as templates. The positions of the N- and C-termini of each domain are indicated. The positions of the conserved motifs discussed in the text (G1, G3, and G4) are found to be identical among the structures. The conserved secondary structure elements are explicitly shown in each domain; the nonconserved parts are depicted as smoothed coils.

The GTPase domain of YjeQ is highly similar to several P-loop GTPases, but has an altered connectivity of the structural elements and associated conserved motifs relative to the typical P-loop-containing GTPase domain (Figure 1C).

Specifically, YjeQ and its orthologs have a circular permutation of the GTPase structure whereby C-terminal strands 5−7 are relocated to the N-terminus to change the signature motif pattern from G1−G3−G4 to G4−G1−G3 (Figure 1C). This circular permutation might have arisen from a tandem duplication of a common ancestral gene with subsequent degradation of the termini. To examine the structural basis and implications of such a permutation, we built a homology model of the GTPase core of YjeQ. To identify the structurally characterized GTPases that are most similar to YjeQ, a position specific score matrix of the YjeQ family was constructed and used to search the PDB database with the PSI-BLAST program. Two GTPases involved in translation, ERA (1EGA) and IF2 (1G7S and 1G7T), were the best hits and were chosen as potential templates for modeling YjeQ. Whole-length alignments of the (predicted) GTPase domains were generated by threading separately the N- and C-terminal parts of YjeQ through the template GTPase structures, and the alignment was optimized by minimizing the mean force potential energy that was computed using a Sippl-like method (*24*). The ERA GTPase (1EGA) provided a good template, with the C-terminal helix coming close to the N-terminal strand of the P-loop motif (G1), which makes circular permutation, as observed in YjeQ, structurally plausible (Figure 1D). The alignments of YjeQ with the templates were submitted for modeling using the PROMODII program, with energy minimization using the GROMOS force field. The core GTPase domain of the translation factor-related GTPase class, which includes several distinct superfamilies of GTPases, such as ERA, IF2, elongation factors, the OBG, and the RAS-like GTPases, contains six conserved strands and four helices (Figure 1D). The model shows that, in the permuted form of the GTPase domain seen in YjeQ and its orthologs, this core is preserved, with the N-terminus of the core located prior to strand 4, instead of the usual strand 1, which precedes the Walker A (G1) motif. The C-terminus of the core, in the permuted domain, lies shortly after the strand that bears the Walker B (G3) motif, which is normally the third strand in the classic GTPase core. The permutation does not disrupt the active site of the GTPase with respect to the relative spatial proximity of the principal nucleotide-binding motif, Walker A (G1), and the magnesium-coordinating, Walker B (G3), suggesting that the permuted proteins retain the catalytic function. Furthermore, despite the permutation, the spatial position of the NKXD (G4) motif, which is the determinant of GTP specificity, relative to the Walker A and Walker B motifs is nearly the same in YjeQ and regular GTPases (Figure 1D), which is compatible with the prediction that YjeQ and its orthologs indeed possess GTPase activity.

The C-terminal portion of YjeQ and its orthologs contains the conserved amino acid pattern Cys-X_4-Cys-X-His-X_5-Cys (X indicates any residue) denoted ZF in Figure 1A. Although this sequence is not significantly similar to other Zn-coordinating cysteine- and histidine-rich domains, the pattern of three conserved cysteines and a conserved histidine is similar to the pattern of conserved residues in the RNA-binding Zn-knuckle domain (*25*), which suggests an analogous mode of divalent metal coordination. As an extension of this analogy, the frequent utilization of Zn clusters in nucleic acid binding suggests that this domain of YjeQ might be a second, in addition to the N-terminal OB-fold domain, determinant of RNA binding in this protein (*26*).

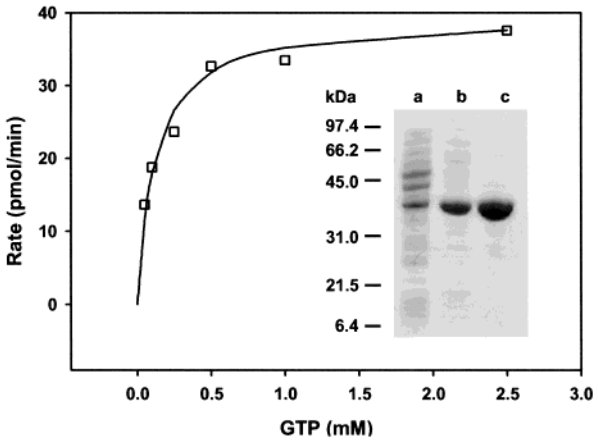

FIGURE 2: Influence of GTP concentration on the rate of phosphate production by YjeQ (untagged). For the rate vs GTP concentration plot, initial rates (average of duplicate determinations) were calculated on the basis of the phosphate produced after a 20 min to 4 h incubation at 23 °C [5.0 μM YjeQ, 50 mM Hepes (pH 7.5) and 10 mM $MgCl_2$]. Incubation times were 20 min for 50 μM GTP, 30 min for 100 μM GTP, 1 h for 250 μM GTP, 1.5 h for 500 μM GTP, 2.5 h for 1 mM GTP, and 4 h for both 2.5 and 5 mM GTP. Values of k_{cat} (9.4 h^{-1}) and K_m (120 μM) were derived from a fit to the Michaelis−Menten equation $V = (k_{cat}/[E])[S]/(K_m + [S])$ by nonlinear regression using SigmaPlot (SPSS, Chicago, IL). The inset shows an SDS−polyacrylamide gel (15% acrylamide) separation for each of three purification steps: the clarified lysate of the overexpressing strain W3110/pLR1 (a, 10 μg), the Q-Sepharose Fast Flow pool (b, 12 μg), and the Superdex 75 pool (c, 15 μg). Samples were denatured by boiling in Laemmli buffer (*36*) containing 8% 2-mercaptoethanol prior to electrophoresis. The apparent molecular mass of purified native YjeQ was 36.5 kDa.

Recombinant, Untagged YjeQ Was Purified Lacking the First 20 Amino Acids. YjeQ was purified to homogeneity in a three-step purification, yielding ~125 mg/L of culture and with purity of ~98% as judged by silver staining. SDS−polyacrylamide gel electrophoresis of the purified protein yielded a molecular mass of 38.5 kDa (Figure 2, inset), significantly smaller than that predicted by the sequence of YjeQ (39 192 Da). Electrospray ionization (ESI) mass spectrometry of the protein yielded a molecular mass of 36 830 Da, a mass consistent with N-terminal amino acid sequencing (data not shown) which showed that the first 20 residues were absent in the purified protein. This stretch of amino acids (^{1}MSKNKLSKGQQRRVNANHQR^{20}) contains a large number of basic residues, does not resemble any known signal sequences, and is conserved among only a subset of YjeQ orthologs (i.e., from *Haemophilus influenzae*, *V. cholerae*, *Pseudomonas aeruginosa*, *Pasteurella multocida*, and *Xylella fastidiosa*). The role of this unique stretch of amino acids is unknown. Placement of an N-terminal histidine tag on YjeQ facilitated the purification of protein with an ESI mass of 41 607 Da, consistent with the expected tagged, full-length YjeQ protein. Whatever its role, the absence of the 20-amino acid peptide from the untagged enzyme did not impact the steady state GTPase activity of YjeQ as measured in this work (Table 1). Both tagged and untagged purified YjeQ behaved as monomers in solution as assessed by size exclusion chromatography on Superdex-75 (Amersham-Pharmacia Biotech) and compared to molecular mass standards (data not shown).

Table 1: Steady State Kinetic Parameters[a] Describing YjeQ[b]

substrate	K_m (mM)	k_{cat} (h^{-1})	k_{cat}/K_m (M^{-1} s^{-1})	fraction[c] of k_{cat}		
				His_6-K220A	His_6-S221A	His_6-K220A/S221A
GTP	0.41 ± 0.1	8.1 ± 0.6	5.5	0.38	0.22	0.052
ATP	1.2 ± 0.2	3.5 ± 0.3	0.8	0.13	0.25	0.12
CTP	2.4 ± 0.9	2.1 ± 0.3	0.2	0.38	0.31	0.12
ITP	1.3 ± 0.3	4.5 ± 0.4	1.0	0.22	0.29	0.093
dGTP	1.6 ± 0.2	7.1 ± 0.3	1.3	0.31	0.19	0.061
dATP	1.0 ± 0.1	5.2 ± 0.2	1.4	0.20	0.22	0.071
GTP[d] (tagless)	0.12 ± 0.1	9.4 ± 0.4	22			
GTP[d] (tagless, S221A)	0.60 ± 0.2	1.8 ± 0.4	0.8			

[a] Nucleotide hydrolysis by pure YjeQ was assessed through measurement of the amount of inorganic phosphate produced using a malachite green/ammonium molybdate colorimetric assay (*20*). YjeQ concentrations were typically 1 μM, and substrate concentrations ranged from 10 μM to 5 mM. Reactions [50 μL, 50 mM Hepes (pH 7.5) and 10 mM $MgCl_2$] were carried out under initial rate conditions (less than 10% of substrate consumed) and allowed to proceed for 20 min to 4 h at 23 °C before being quenched with malachite green/ammonium molybdate reagent for phosphate analysis. Values of k_{cat} and K_m were derived from a fit to $V = (k_{cat}/[E])[S]/(K_m + [S])$ by nonlinear regression where errors are the standard error of fit. [b] Unless otherwise indicated, parameters are reported for His-tagged YjeQ purified as described in Materials and Methods. [c] Site-directed variants of YjeQ (His-tagged) were tested for nucleotidase activity at 5 mM nucleoside triphosphate. Activities are reported as a fraction of k_{cat} for the wild-type His-tagged enzyme. [d] Parameters describing the steady state GTPase of tagless YjeQ and YjeQ S221A.

YjeQ Catalyzes Slow Hydrolysis of GTP and Other Nucleotides. Steady state kinetic analysis of nucleotide hydrolysis by both purified tagged and untagged YjeQ revealed slow but saturable turnover of GTP with the production of inorganic phosphate (Figure 2 and Table 1). Values of k_{cat} and K_m were 8.1 h^{-1} and 0.41 mM for His-tagged YjeQ and 9.4 h^{-1} and 0.12 mM for untagged YjeQ, respectively. The steady state rate of GTP hydrolysis observed with YjeQ is comparable to those of p21H-Ras and *E. coli* EF-Tu, which have intrinsic GTPase turnover numbers of 1.7 and 2.2 h^{-1}, respectively (*27*, *28*).

YjeQ exhibited relatively broad substrate specificity in the steady state, hydrolyzing other nucleotide substrates with catalytic efficiencies that were as little as 5-fold lower than that of GTP (k_{cat}/K_m values of 0.8, 0.2, 1.0, 1.4, and 1.3 for ATP, CTP, ITP, dATP, and dGTP, respectively) with His-tagged enzyme (Table 1). Interestingly, the K_m values for tagged and untagged YjeQ for GTP (0.41 and 0.12 mM, respectively) were consistent with the known cellular concentration of GTP (0.39 mM) in *E. coli* K12 cells (*29*). In contrast, K_m values for all other nucleoside triphosphates were greater than 1 mM. In the case of ATP, for example, the K_m value of 1.2 mM is approximately 4 times the physiological concentration (0.31 mM) in *E. coli* (*29*).

That the tagged and untagged enzymes exhibited similar k_{cat} and K_m values, despite having been prepared with fundamentally different chromatographic strategies, suggested that the steady state GTPase was not due to a minor contaminant in each of the preparations. We further attempted to address the issue of background NTPase activity through the construction of His-tagged site-directed variants in YjeQ (K220A, S221A, and the double variant K220A/S221A), with substitutions in the P-loop. The equivalent residues in the active sites of Ras (K16 and S17) and Gs_α (K53 and S54) have a critical catalytic role in coordinating active site Mg^{2+} (*30*−*32*). An analysis in the steady state of each of the variants was performed at a saturating nucleotide concentration (5 mM) and described in Table 1 as a fraction of the k_{cat} observed with purified His-YjeQ (Table 1). Variants Lys220Ala and Ser221Ala were significantly impaired in steady state nucleotide hydrolysis, retaining 13−38 and 19−30% of maximal velocity against a variety of nucleoside triphosphates, respectively. The double variant K220A/S221A was further impaired showing residual activities of 6−12% of V_{max} against the nucleotides that were tested. From these experiments, it can be inferred that less than 12% of the observed steady state rates of NTP hydrolysis by His-YjeQ was due to contaminating NTPases.

In control experiments aimed at establishing background nucleoside triphosphate hydrolysis rates that may originate from proteins that copurify with tagged or untagged YjeQ, we carried out assays on samples from mock purifications as described in Materials and Methods. For the tagged and untagged mock purifications, sample volumes were adjusted to be consistent with 1 μM YjeQ in the original protocols. In a 4 h incubation with 2.5 mM nucleotide, we were unable to detect the production of inorganic phosphate with any of the nucleotides listed in Table 1. We estimate that this assay is sensitive to greater than 3 pmol/h. With active YjeQ (50 μL of a 1 μM solution, 50 pmol), steady state rates ranged from 102 (CTP) to 470 pmol/h (GTP) (k_{cat} values of 2.1 and 9.4 h^{-1}, respectively). Therefore, our purified tagged and untagged YjeQ samples have background nucleotidase activities with magnitudes that are negligible compared with the observed rates (<3%).

Purified YjeQ Binds GDP. To test for bound substrates, purified YjeQ was quenched with 0.2 N NaOH and filtered through a 5000 Da cutoff filter to remove the denatured enzyme and the filtrate neutralized by the addition of HCl prior to analysis using paired ion chromatography as described in Materials and Methods. Detection at 271 nm indicated the presence of a species that comigrated with GDP in this solvent system (data not shown). We estimated 0.6 equiv of nucleotide bound to the purified enzyme through comparison with a standard curve of GDP. Analysis of the bound nucleotide by electrospray ionization mass spectrometry yielded a molecule mass of 442.0 Da (data not shown), in good agreement with that expected for GDP (442.1 Da). Efforts to remove the bound nucleotide and retain GTPase activity were unsuccessful. Dialysis, for example, with 20 mM EDTA, followed by dialysis to remove EDTA and restore Mg^{2+} to 10 mM in buffer abolished hydrolytic activity (data not shown). Bound GDP therefore appeared to be critical to the stability of purified YjeQ, a property common to many GTPases, including H-Ras (*33*) and EF-Tu (*34*). The nucleotide binding activity of the purified enzyme was

also assessed with [^{35}S]GTPγS using a standard glass microfiber filter binding assay. That analysis demonstrated that 0.6 equiv of YjeQ was bound by [^{35}S]GTPγS after incubation for 2 h (data not shown). In aggregate, these experiments suggested that an active fraction (60%) of YjeQ was purified with tightly bound GDP and that a similar fraction was competent for exchange with [^{35}S]GTPγS.

YjeQ Exhibits a Burst in GTP Hydrolysis. Pre-steady state kinetic analysis of YjeQ was complicated by the finding that YjeQ purified with 0.6 equiv of bound GDP and that removal of GDP by an extensive 48 h dialysis abolished enzyme activity. Nevertheless, rapid mixing and quench experiments were performed on a time scale of 2.3 ms to 1.6 s and followed by HPLC to examine the course of the reaction in the presence of saturating GTP (5 mM) and using high concentrations of enzyme (400−800 μM). A millisecond time scale burst of GDP production was observed in these experiments (Figure 3A). The burst exponential was characterized by first-order rate constants that were not dependent on the amount of enzyme that was added (105, 93, and 95 s^{-1} at 400, 600, and 800 μM enzyme, respectively). The steady state rate (k_2) for these time courses was linear with enzyme concentration (Figure 3B) and was described by a steady state turnover rate of 8 h^{-1} (slope of Figure 3B) similar to that seen for k_{cat} using steady state kinetics (9.4 h^{-1}). The amplitude of the burst was also linear with the amount of enzyme that was added and was characterized by a burst amplitude that was 0.12 equiv of YjeQ added (Figure 3C). Given that the purified enzyme was bound by 0.6 equiv of nucleotide, it is not surprising that the burst was less than stoichiometric. On the other hand, it is curious that we saw any burst at all since removal of bound nucleotide by exhaustive dialysis with EDTA abolished enzyme activity. It must be that a significant fraction, namely, 12%, of the purified enzyme was not bound by nucleotide and remained catalytically active. Thus, pre-steady state rapid quench experiments with GTP indicated that YjeQ catalyzed the rapid hydrolysis of GTP (100 s^{-1}) at a rate that was 45 000 times greater than that of steady state turnover (8 h^{-1}).

Pre-steady state kinetics with ATP also showed a burst of ATP hydrolysis followed by a slow steady state rate (Figure 4). In contrast to the rapid rate of hydrolysis observed for GTP, a much slower burst exponential (k_1) was observed for ATP (0.2 s^{-1}), suggesting a kinetic preference at saturating substrates of nearly 500-fold for GTP (Figure 4). The amplitude of burst seen with ATP was 28 nmol from 198 nmol of enzyme or 0.14 equiv, similar in magnitude to that observed for GTP. The steady state rate (k_2) was found to be 0.21 nmol/s, equivalent to a turnover of 3.8 h^{-1} and similar to that determined using steady state kinetics (3.6 h^{-1}, Table 1). The large quantities of enzyme required for pre-steady state experiments were prohibitive with respect to an exploration of the kinetics of hydrolysis of other substrates investigated in the steady state. Even so, a reasonable conclusion of the experiments presented here is that the specificity of YjeQ is manifested in the presteady state where hydrolysis of GTP occurs at rates far in excess of those for other nucleotides.

Finally, we were interested in further characterizing the S221A variant using pre-steady state techniques primarily because this putative active site variant demonstrated steady state turnover that was reduced in magnitude only 5-fold relative to that seen for the wild-type enzyme despite a presumed role in coordinating an active site magnesium (Figure 5, inset). Again, we saw burst kinetics from this variant (Figure 5) with a rate constant for hydrolysis (k_1) of 0.3 s^{-1}, reduced 300-fold relative to that of the wild-type enzyme. The amplitude of the burst was 0.09 equiv (22 nmol of GDP from 246 nmol of enzyme), and the steady state rate (k_2) was determined to be 0.19 nmol/s. The latter translates to a turnover at saturating GTP of 2.8 h^{-1}, similar to that determined using steady state kinetics (1.8 h^{-1}, Table 1).

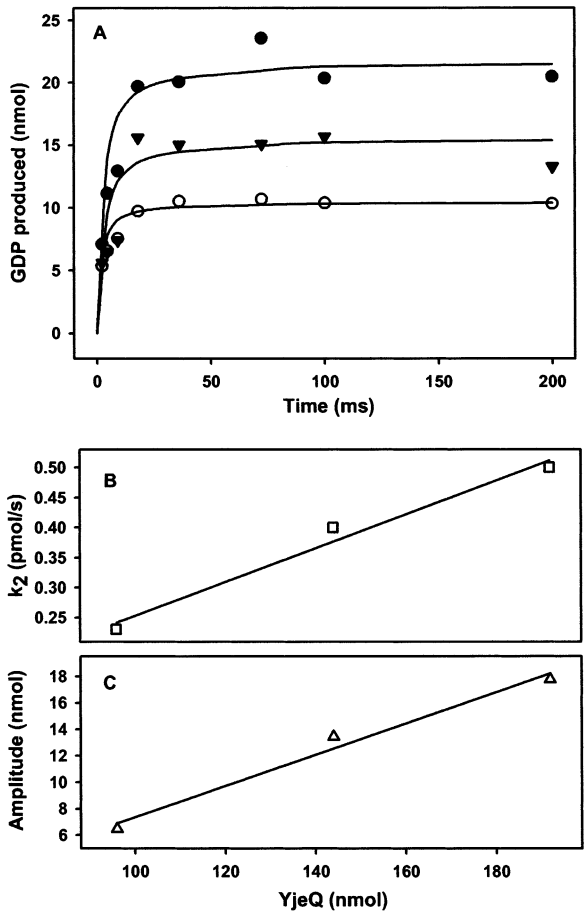

FIGURE 3: Analysis of burst kinetics of GTP hydrolysis by YjeQ. Solutions were mixed and reactions quenched as described in Materials and Methods. The top panel shows the time course for rapid mixing experiments using a three-syringe method where 112 μL of substrate (e.g., 5 mM [α-^{32}P]GTP, 4 Ci/mol) was mixed with 112 μL of enzyme [800 (○), 1200 (▼), and 1600 μM (●)] and allowed to react for 2.3 ms to 120 s before the reaction was quenched with the addition of 112 μL of 0.6 N NaOH (data shown are from 2.3 to 200 ms). GDP production was monitored by HPLC with in-line radioactivity detection as described in Materials and Methods. Each point is the average of three quench experiments, and curves are best fits of the data to eq 1. Calculated burst rates (k_1) were 105 (○), 93 (▼), and 95 s^{-1} (●). The bottom panel illustrates the linear relationship between both the steady state rate (k_2) and burst amplitude with YjeQ added. The slope of k_2 vs YjeQ yielded a turnover at saturating GTP (k_{cat}) of 8 h^{-1}. The slope of amplitude vs YjeQ yielded a burst fraction of 0.12.

DISCUSSION

Protein sequence and structure analysis of YjeQ, an essential *E. coli* protein of unknown function (*6*), resulted in the testable hypothesis that YjeQ is a circularly permuted GTPase. YjeQ and its orthologs are widespread in bacteria

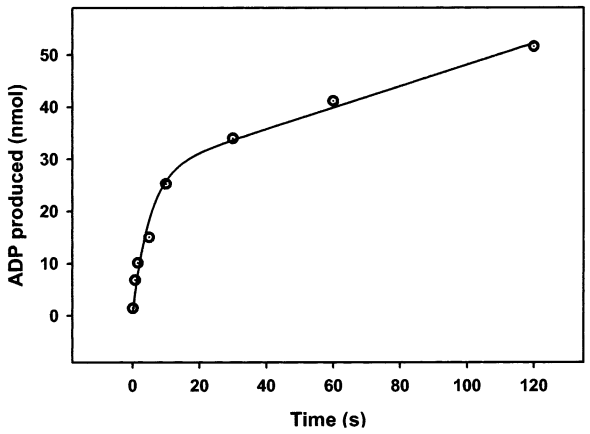

FIGURE 4: Burst analysis with ATP as a substrate. Shown are time courses for hydrolysis of ATP by YjeQ using a three-syringe method where 120 μL of ATP (6 mM [α-^{32}P]ATP, 2.6 Ci/mol) was mixed with 120 μL of enzyme (1770 μM) and allowed to react for 100 ms to 2 min before the reaction was quenched with the addition of 120 μL of 0.6 N NaOH. ADP was monitored by HPLC with in-line radioactivity detection as described in Materials and Methods. Each point is the average of three quench experiments, and curves are best fits of the data to eq 1 that yielded the following parameters: $a = 28$ nmol (amplitude), $k_1 = 0.19$ s^{-1} (burst rate), and $k_2 = 0.21$ nmol/s (steady state rate).

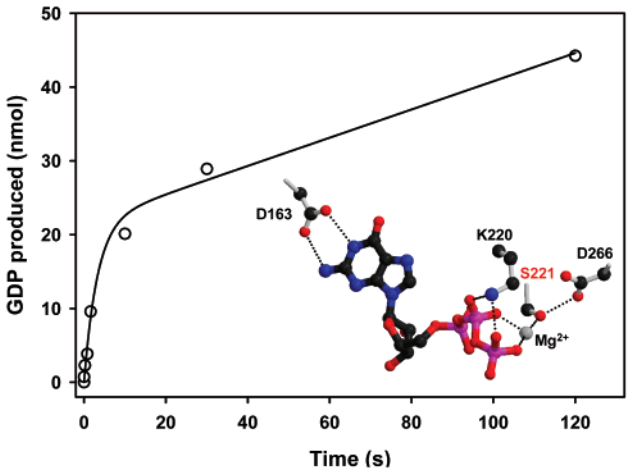

FIGURE 5: Burst analysis of the S221A variant. Shown are the time courses for hydrolysis of GTP using a three-syringe method where 112 μL of GTP (5 mM [α-^{32}P]GTP, 2.6 Ci/mol) was mixed with 112 μL of enzyme (2200 μM) and allowed to react for 2.3 ms to 120 s before the reaction was quenched by addition of 112 μL of 0.6 N NaOH. GDP production was monitored by HPLC with in-line radioactivity detection as described in Materials and Methods. Each point is the average of three quench experiments, and curves are best fits of the data to eq 1 that yielded the following parameters: $a = 22$ nmol (amplitude), $k_1 = 0.30$ s^{-1} (burst rate), and $k_2 = 0.19$ nmol/s (steady state rate). The inset highlights key residues, based on homology modeling with h-Ras (*29*), thought to be in the proximity of bound GTP in the active site of YjeQ (i.e., S221 in YjeQ, which is equivalent to S17 in Ras).

(*7*, *8*) and belong to a larger superfamily of GTPases that contain a permuted arrangement of signature GTPase motifs and are nearly universally present in the three primary kingdoms of life, bacteria, archaea, and eukaryotes (*5*). Thus, YjeQ might serve as a prototype in understanding the functions of a widespread but uncharacterized group of GTPases that probably perform fundamental functions in a wide range of organisms. Homology modeling of the predicted GTPase domain of YjeQ (residues 121−271) suggested that, despite the permutation, the core of this was likely to preserve its usual conformation and retain catalytic activity. Therefore, in this work, we experimentally examined the prediction that YjeQ is a GTPase.

Steady state analysis revealed that YjeQ catalyzed the slow hydrolysis of GTP ($k_{cat} \sim 9$ h^{-1}) as well as other nucleotides without a strong specificity for its presumed substrate, GTP. Variants K220A and S221A, with substitutions presumed to interfere with the coordination of the Mg^{2+} in the active site of YjeQ, were reduced only ~2.5- and ~5-fold, respectively, in GTPase at saturating GTP. Moreover, the double variant K220A/S221A was reduced about 20-fold in GTPase. Conversely, substitutions of the equivalent serine, for example, in h-Ras (S17) resulted in a significant reduction in the rate for GTPase to rates that were not measurable in the presence or absence of GTPase activating protein (*32*). Thus, our steady state analysis was somewhat inconclusive in demonstrating the GTPase function of YjeQ.

Transient kinetic analysis of the GTPase of YjeQ demonstrated a burst in the formation of GDP and inorganic phosphate at the active site of YjeQ, where the rate of the burst (100 s^{-1}) was 45 000 times greater than that of turnover. In further contrast to our steady state analysis, the burst in GTP hydrolysis was specific for GTP (480-fold faster than for ATP) and highly sensitive to the S221A substitution (300-fold slower). Thus, the turnover of YjeQ appeared to be primarily influenced by product release. The fact that YjeQ was also found to copurify with bound GDP leads us to speculate that turnover may be limited, in particular, by a very slow rate of release for GDP.

In sum, the work presented here suggests that YjeQ is a GTPase that, in isolation, performs hydrolysis and turnover of GTP at remarkably different rates. We believe that these findings have predictive power in designing further experiments directed at determining the biochemical and physiological details of the function of YjeQ. These findings are consistent with a role for YjeQ that involves the transduction of the energy of hydrolysis of GTP into mechanical work. Sequence analysis of YjeQ and its orthologs revealed potential accessory domains, namely, the N-terminal S1-like OB-fold domain and the C-terminal Zn finger, which could function in such a transduction process through interactions with other macromolecules, in particular RNA. Given the presence of these domains and the fact that many GTPases, particularly those that are highly conserved during evolution, function in translation, it appears likely that YjeQ is an unknown, bacteria specific translation factor. The demonstration of the GTPase activity of YjeQ defines a biochemical basis for further investigation of the function of this important bacterial protein of unknown function.

ACKNOWLEDGMENT

We thank Janid Ali and Gerry Wright for thoughtful comments on the science and on the manuscript.

REFERENCES

1. Saraste, M., Sibbald, P. R., and Wittinghofer, A. (1990) *Trends Biochem. Sci. 15*, 430−434.
2. Vetter, I. R., and Wittinghofer, A. (1999) *Q. Rev. Biophys. 32*, 1−56.
3. Dever, T. E., Glynias, M. J., and Merrick, W. C. (1987) *Proc. Natl. Acad. Sci. U.S.A. 84*, 1814−1818.
4. Bourne, H. R., Sanders, D. A., and McCormick, F. (1991) *Nature 349*, 117−127.

5. Leipe, D. D., Koonin, E. V., and Aravind, L. (2002) *J. Mol. Biol.* (in press).
6. Arigoni, F., Talabot, F., Peitsch, M., Edgerton, M. D., Meldrum, E., Allet, E., Fish, R., Jamotte, T., Curchod, M. L., and Loferer, H. (1998) *Nat. Biotechnol. 16*, 851−856.
7. Tatusov, R. L., Koonin, E. V., and Lipman, D. J. (1997) *Science 278*, 631−637.
8. Tatusov, R. L., Natale, D. A., Garkavtsev, I. V., Tatusova, T. A., Shankavaram, U. T., Rao, B. S., Kiryutin, B., Galperin, M. Y., Fedorova, N. D., and Koonin, E. V. (2001) *Nucleic Acids Res. 29*, 22−28.
9. Heinemann, U., and Hahn, M. (1995) *Prog. Biophys. Mol. Biol. 64*, 121−143.
10. Ponting, C. P., and Russell, R. B. (1995) *Trends Biochem. Sci. 20*, 179−180.
11. Jeltsch, A. (1999) *J. Mol. Evol. 49*, 161−164.
12. Bujnicki, J. M. (2000) *Int. J. Biol. Macromol. 27*, 195−204.
13. Altschul, S. F., Madden, T. L., Schaffer, A. A., Zhang, J., Zhang, Z., Miller, W., and Lipman, D. J. (1997) *Nucleic Acids Res. 25*, 3389−3402.
14. Notredame, C., Higgins, D. G., and Heringa, J. (2000) *J. Mol. Biol. 302*, 205−217.
15. Kaplan, W., and Littlejohn, T. G. (2001) *Briefings Bioinf. 2*, 195−197.
16. Kraulis, P. J. (1991) *J. Appl. Crystallogr. 24*, 946−950.
17. Daigle, D. M., Hughes, D. W., and Wright, G. D. (1999) *Chem. Biol. 6*, 99−110.
18. Gill, S. C., and von Hippel, P. H. (1989) *Anal. Biochem. 182*, 319−326.
19. Weiland, T., and Jakobs, K. H. (1994) *Methods Enzymol. 237*, 3−13.
20. Lanzetta, P. A., Alvaez, L. J., Reinach, P. S., and Candia, O. A. (1979) *Anal. Biochem. 100*, 95−97.
21. Allinquant, B., Musenger, C., and Schuller, E. (1985) *J. Chromatogr. 326*, 281−291.
22. Murzin, A. G. (1993) *EMBO J. 12*, 861−867.
23. Draper, D. E., and Reynaldo, L. P. (1999) *Nucleic Acids Res. 27*, 381−388.
24. Sippl, M. J. (1990) *J. Mol. Biol. 213*, 859−883.
25. De Guzman, R. N., Wu, Z. R., Stalling, C. C., Pappalardo, L., Borer, P. N., and Summers, M. F. (1998) *Science 279*, 384−388.
26. Laity, J. H., Lee, B. M., and Wright, P. E. (2001) *Curr. Opin. Struct. Biol. 11*, 39−46.
27. Frech, M., Darden, T. A., Pedersen, L. G., Foley, C. K., Charifson, P. S., Anderson, M. W., and Wittinghofer, A. (1994) *Biochemistry 33*, 3237−3244.
28. Rutthard, H., Anindya, B., and Makinen, M. W. (2001) *J. Biol. Chem. 276*, 18728−18733.
29. Buchholz, A., Takors, R., and Wandrey, C. (2001) *Anal. Biochem. 295*, 129−137.
30. Pai, E. F., Krengel, U., Petsko, G. A., Goody, R. S., Kabsch, W., and Wittinghofer, A. (1990) *EMBO J. 9*, 2351−2359.
31. Hildebrandt, J. D., Day, R., Farnsworth, C. L., and Feig, L. A. (1991) *Mol. Cell. Biol. 11*, 4830−4838.
32. John, J., Rensland, H., Schlichting, I., Vetter, I., Borasio, G. D., Goody, R. S., and Wittinghofer, A. (1993) *J. Biol. Chem. 268*, 923−929.
33. Zhang, J., and Matthews, C. R. (1998) *Biochemistry 37*, 14891−14899.
34. Rutthard, H., Banerjee, A., and Makinen, M. W. (2001) *J. Biol. Chem. 276*, 18728−18733.
35. Merritt, E. A., and Murphy, M. E. P. (1994) *Acta Crystallogr. D50*, 869−873.
36. Laemmli, U. K. (1970) *Nature 227*, 680−685.

BI020355Q